

ECE 469

Lab Report - 5

Debojyoti Mazumdar¹ and Sebastian Armstrong²

¹Electrical and Computer Engineering, UIUC

²Electrical and Computer Engineering, UIUC

Abstract—Labs 9, 10, and 11 focuses on using the power board, interface board, and Arduino to generate PWM, implement digital current control for a buck converter, and perform MPPT for a solar panel.

I. DISCUSSION OF EXPERIMENT-9

A. Theory

1) *Dead-time generation*: The circuit used to generate the dead-time is shown in Figure-1.

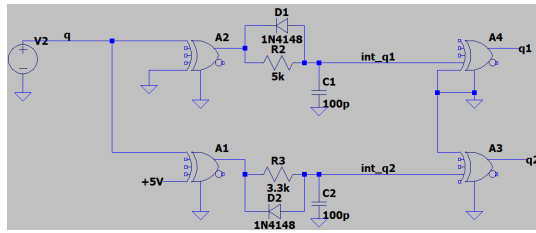


Fig. 1: Circuit diagram for generating dead-time.

The working of the circuit uses the RC charging delay to generate the delay¹. Increasing the resistance of the RC circuit would lead to more delay for the voltage across the capacitor to reach its maximum. The diode provides a quick discharge path from the capacitor through the ground connection of the XOR gate, without causing any delay². This is because we want a delay only in the rising edge of the signal and not falling edge. We would like the dead-time to be equal to the sum of turn-off delay time ($t_{d(off)}$) and fall time (t_f)³. This is because this sum is more than the sum of rise time (t_r) and turn-on delay time ($t_{d(on)}$). If we keep the dead-time more than necessary, it would lead to more loss of input power⁴. The dead-time (t_d) is as shown below⁵.

$$t_d = RC \times \log(2) \quad (1)$$

B. Lab 9 results

First we checked the working of the PWM generator. We got the PWM waveform and sawtooth waveform as shown in Figures - 2 and 3.



Fig. 2: PWM output and sawtooth output with switching frequency of 100 kHz and duty ratio of 25 %



Fig. 3: PWM output and sawtooth output with switching frequency of 100 kHz and duty ratio of 50 %

We then checked the dead-time generation of the two signals $q_1(t)$ and $q_2(t)$. We generated a dead-time of 250 ns between $q_1(t)$ and $q_2(t)$ by changing the value of the resistances $Rdt1$ and $Rdt2$. Figures - 4 and 5 shows the dead-time generated.

Then we ran the synchronous and regular buck converter and obtained the efficiency in each case. Table- shows the values of input power (P_{in}), output power (P_{out}) and the efficiency.

As can be seen from the tables, the efficiency is more for the regular buck converter than the synchronous buck converter. This is because of the fact that dead-time actually reduces the power lost by reducing switching losses.

¹Answer to Study Question-1

²Answer to Study Question-2

³Answer to Study Question - 3

⁴Answer to Study Question - 4

⁵Answer to Study Question - 5



Fig. 4: time delay between the falling edge of $q_1(t)$ and $q_2(t)$.

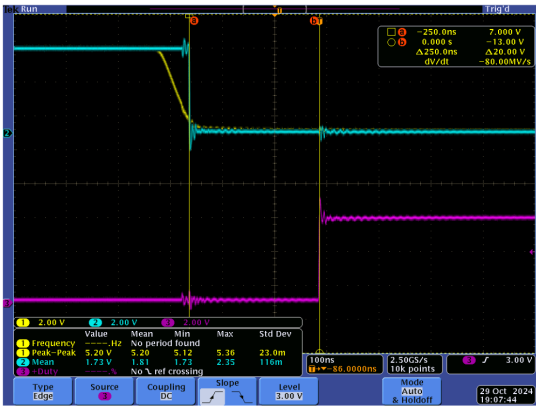


Fig. 5: time delay between the falling edge of $q_2(t)$ and rising edge of $q_1(t)$.

D	P_{in} (W)	P_{out} (W)	Efficiency (%)
0.25	10.8	1.6	14.8
0.5	12.45	6.963	55.9

TABLE I: Table of input power (P_{in}), output power (P_{out}) and efficiency for different values of duty cycle (D) for the synchronous buck converter.

D	P_{in} (W)	P_{out} (W)	Efficiency (%)
0.25	2.31	1.42	61.47
0.5	8.35	6.772	81.11

TABLE II: Table of input power (P_{in}), output power (P_{out}) and efficiency for different values of duty cycle (D) for the regular buck converter.

II. DISCUSSION OF EXPERIMENT-10

A. Results

1) *Voltage and current measurement calibration:* The voltage sensors and current sensor, which utilize the ADCs on the Arduino, were calibrated by measuring three operating conditions for the synchronous buck converter. The actual value was recorded using a scope while the ADC reading was printed to serial monitor.

The results of the calibration are plotted in Figs. 6, 7, and 8.

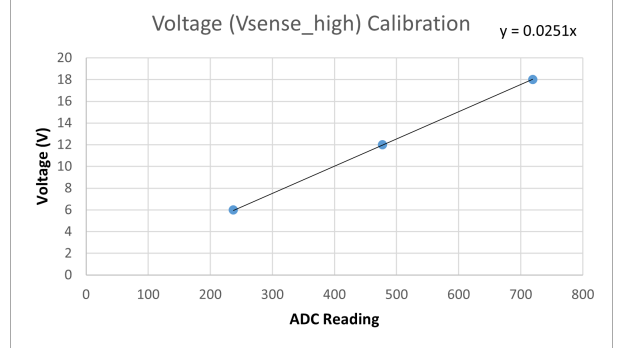


Fig. 6: Voltage vs 10-bit ADC reading for calibration of the V_{high} sensor.

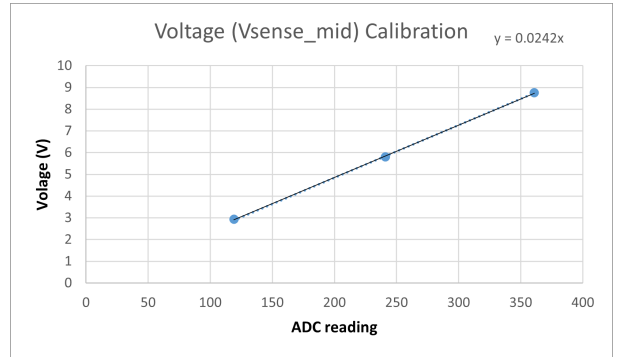


Fig. 7: Voltage vs 10-bit ADC reading for calibration of the V_{mid} sensor.

2) *Open loop and closed loop control:* The buck converter was first tested in "mode 1," in which a potentiometer adjusted the duty cycle D . Results for manually adjusting D to keep the inductor current at 1 A are shown in Table III. Two test cases considered the effects of input voltage changing to 18 V or the load resistance increase by 2x.

TABLE III: Results from open-loop control of inductor current. The nominal duty cycle $D_{nom} = 0.64$, which results in 1 A for the first test case.

V_{in} (V)	R_L (Ω)	i_L at D_{nom} (A)	D for $i_L = 1$ A
12	7.5	1	0.64 (D_{nom})
18	7.5	1.51	0.417
12	15	0.52	0.95

Next, a proportional controller was tested. Various gains were evaluated for tracking a reference inductor current of 1 A. Results are shown in Table IV. Lastly, PI control was evaluated for the tuning $k_p = 0.5$ and $k_i = 0.01$. Various input voltages were tested ranging from 4 to 18 V. Results for the PI controller are shown in Table V.

TABLE IV: Performance of P controller at various proportional gains.

K_p	i_L (A)	D
0.1	0.11	0.09
0.5	0.4	0.25 - 0.36
1	0.57	0.2 - 0.5
10	0.85	0.06 - 0.95

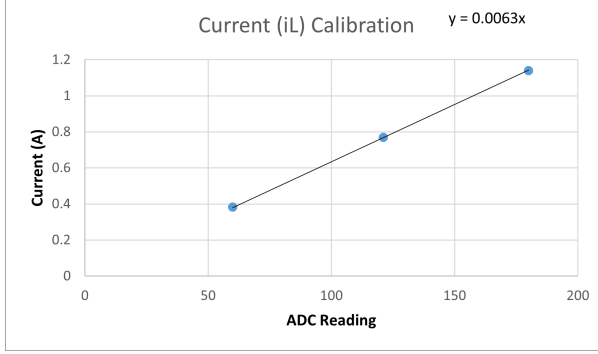


Fig. 8: Current vs 10-bit ADC reading for calibration of the i_L sensor.

TABLE V: Performance of PI controller at various input voltages.

V_{in} (V)	i_L (A)	D
4	0.475	0.95
8	0.97	0.95
12	-	0.61 - 0.72
16	0.9 - 1.13	0.38 - 0.56
18	0.86 - 1.12	0.2 - 0.5

The closed loop controllers exhibited oscillations in duty cycle which did not occur for the open-loop cases. For the 18 V case for the PI controller, we noticed the duty cycle oscillated between 0.2 to 0.5, which includes the value found earlier in the open loop test ($D = 0.417$ for $i_L = 1$ A). For the light load case, both the PI controller and the open-loop control went into saturation, with $D = 0.95$ and $i_L \approx 0.75$ A.⁶

Considering the $V_{in} = 4$ V case, we can again see that the duty cycle saturates at 0.95. For such a low input voltage, it is not possible to supply the required output voltage across the load for $i_L = 1$ A.⁷

Comparing the performance of the P and PI controllers, we see that the P controller has significant steady-state error between the reference current and measured current. This error is worse for lower k_p . However, in order to reduce the error down to 0.15 A, the k_p value must be made overly aggressive—in fact, the duty cycle oscillated between 0.06 and 0.95 for $k_p = 10$. The integral term of the PI controller addresses this drawback. A much lower gain of $k_p = 0.5$ can be used while the integral term cancels out any steady-state error. For example, at $V_{in} = 16$ V, the inductor current stayed within 0.9 to 1.13 A with only an oscillation in D from 0.38 to 0.56.⁸

III. DISCUSSION OF EXPERIMENT 11: SOLAR MPPT

A. Theory of solar PV system with MPPT

Solar photovoltaics (PV) are becoming widely deploying in grids to supply electricity. Solar energy benefits from zero fuel cost and drastically reduced carbon emissions compared to fossil fuel based power generation.

In this experiment, we will delve into the process of extracting power from a solar PV panel, which is comprised of many individual PV cells.

Figure 9 shows the I-V characteristic for a typical solar panel. For much of the I-V characteristic, a PV cell behaves roughly like a current source; however, as the load on the PV cell becomes sufficiently light, the current will decrease as the voltage continues to increase. Close to the open circuit (the maximum) voltage of the cell, it behaves like a voltage source⁹.

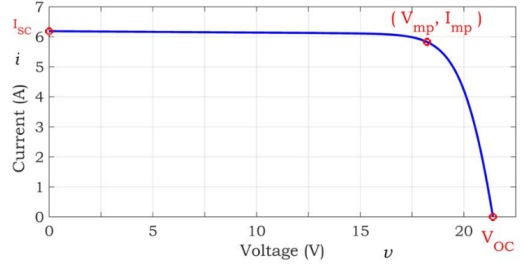


Fig. 9: Current-Voltage characteristic for a PV panel. Source: [1]

Note that there is a particular point on the I-V characteristic at which the area of $V \times I$ is maximized. This point is known at the maximum power point (MPP), since maximum power can be extracted here.

The MPP depends on solar irradiance and the temperature of the PV cell. Due to these factors, it is desirable to use control to track the operating point at which maximum power can be extracted, and this process is called maximum power point tracking (MPPT).

MPPT allows tracking of the optimal power to match changes in irradiance, which can occur due to cloud cover. Infact, a PV panel can exhibit very rapid changes in power output due to shading, on the order of its full rated power capacity each second [2].

1) *the effect of varying load resistance:* Varying the effective load seen by the PV panel allows for tracking of the MPP. A resistor has a linear I-V characteristic, which will intercept with the PV characteristic at some point. A smaller resistance value will draw more current, up to the short circuit current. On the other hand, a larger resistance will draw less current and the voltage will rise, up to the maximum of the open-circuit voltage. There will be an optimal resistance that results in the voltage and current for maximum power extraction.

In practice, a controller cannot vary a physical resistor, instead a power electronic converter is utilized. Consider the

⁶Answer to lab 10 study question 1

⁷Answer to lab 10 study question 2

⁸Answer to lab 10 study question 3

⁹Answer to lab 11 study Q1

case of a buck converter as shown in the following circuit in Fig. 10.

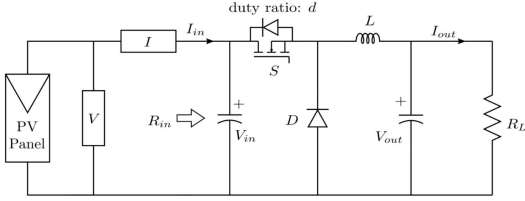


Fig. 10: PV panel connected to a buck converter and resistive load. Source: [1]

The resistance “seen” by the PV panel looking into the buck converter will be the ratio V_{in}/I_{in} .

Given that $V_{out}/I_{out} = R_L$, and $V_{out} = DV_{in}$ (from volt-second balance), and $I_{in} = DI_{out}$ (from power balance), we can solve for the effective input resistance.

$$\begin{aligned} R_{in} &= V_{in}/I_{in} \\ &= \frac{V_{out}}{D} \frac{1}{DI_{out}} \\ &= R_L/D^2 \end{aligned}$$

Thus, by varying D we can change R_{in} from R_L to ∞ (since D must be between 0 and 1).

2) *MPPT using boost converter:* If we wanted to vary R_{in} below R_L , we would need to use a different power electronic converter. A boost converter works for this purpose, as discussed below.

For a boost converter, we have the following relationships:

$$\begin{aligned} V_{out} &= \frac{V_{in}}{1-D} \\ I_{in} &= \frac{I_{out}}{1-D} \end{aligned}$$

Solving for R_{in} , we get the following:

$$\begin{aligned} R_{in} &= V_{in}/I_{in} \\ &= \frac{V_{out}(1-D)(1-D)}{I_{out}} \\ &= R_L(1-D)^2 \end{aligned}$$

Thus, we can see that for a boost converter, the effective load resistance can be varied between $R_{in} \in [0, R_L]$.¹⁰

3) *Perturb and Observe Control:* To track the maximum power point, we need a way to dynamically change the duty cycle whenever the irradiance or temperature of the PV panel changes. In general, an open-loop controller is not feasible, and we would like to avoid the cost of adding sensors to measure solar flux and panel temperature. We can employ a feedback mechanism to measure the output power and adjust the duty cycle until the power reaches the MPP; a common technique is called “perturb and observe” (P&O). In P&O, the duty cycle is incremented by a small amount and the output power is measured. If the power is seen to increase, the duty

cycle will be incremented again in the same direction. However, if the power decreases, the increment reverses direction. In this sense, the duty cycle will be adjusted incrementally until it oscillates back-and-forth about the optimal duty cycle for maximum power extraction. A block diagram for P&O control is shown in Fig. 11. If the solar irradiance changes, the algorithm will automatically sense a change in power output and the duty cycle will be adjusted accordingly.

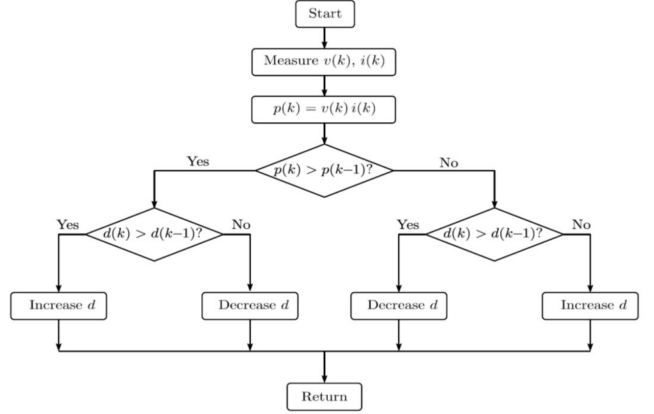


Fig. 11: Block diagram of Perturb and Observe algorithm. Source: [1]

4) *Beyond basic MPPT with a resistive load:* In many applications, we want to use a PV panel to charge a battery. This could occur for a small microgrid system or a utility-scale PV-BESS installation. If we consider a battery as a load in place of a resistor, do we need to modify the P&O algorithm?

If we assume a buck converter topology and that the battery voltage is below the PV panel voltage, then we can implement the same P&O algorithm without any modifications. Although the load is no longer resistive, varying the duty cycle will still change the effective voltage looking into the buck converter, as given by $V_{in} = V_{batt}/D$.

This relationship will result in an intersection with the MPP, provided that the required $V_{in(MPP)} > V_{batt}$.

If the V_{in} were to drop below V_{batt} , the buck converter will cease functioning correctly (body diode on MOSFET will turn on). The battery will try to supply power into the solar panel, which is not desired. To prevent this, a diode could be added to prevent reverse current flow—or a boost converter could be used in place of the buck converter (which comes with a diode for free).

In addition, an alternative controller could be implemented by using an inner current control loop and outer MPPT loop. The current loop would be based on a PI controller that modifies the duty cycle to achieve a reference output current. The outer MPPT loop would modify the reference current based on a P&O algorithm. Each cycle of the P&O would step the reference current by a small ΔI_{out} . This approach would be well suited for a battery charging application, since the reference current could be limited to stay within the safe operating regime for the battery.¹¹

¹⁰Answer to study question 4 for lab 11

¹¹Answer to study question 2 for lab 11

In some cases, MPPT may not be the desired control objective. Consider a 1 MW utility solar farm. From the perspective of the power system, it is desirable that the solar farm provides a consistent power output—for grid reliability and system stability. As mentioned previously, such a farm could exhibit ramp rates up to 1 MW/s [2]. Typically, a battery storage system (BESS) is required to smooth out the variability of the PV.

According to [2], a modified control approach for the power electronics could aid in smoothing the power output by derating the PV system slightly below the MPP. Doing so results in 5x less BESS capacity requirement. Moreover, derating the solar farm below the maximum power point provides a reserve in power generation, similar to a “spinning reserve,” which enables the solar farm to provide ancillary services to the power system.¹²

In addition, as power systems experience higher penetrations of renewables, it will become necessary to curtail power generation at certain time periods when generation exceeds the demand.

B. Methods

We used solar panel no. 47 on the roof of ECEB. Several of the solar panels are accessible via cables connected to the lab. In our experiment, we only used 1/4 of an entire panel in order to operate at a safer voltage level. The solar panel used is shown in Fig. 12 below.



Fig. 12: Solar panel 47, used in this experiment.

We configured the power board to operate as a synchronous buck converter, with digital control using the Arduino and interface board. A sketch of the schematic (including probe measurement points), is shown in Fig. 13.

Originally, we started with a load resistance of $R_L = 15 \Omega$, but this value was too large. We eventually strung six 2Ω resistors in parallel to create a low load resistance (i.e., $R_L = 0.33$). It's possible that this system could have performed better using a boost converter, since a boost converter allows lowering of the effective load resistance below R_L . In addition, a lamp was connected in series with R_L to provide a visual indicator of the power output from the PV panel. The lamp has a resistance

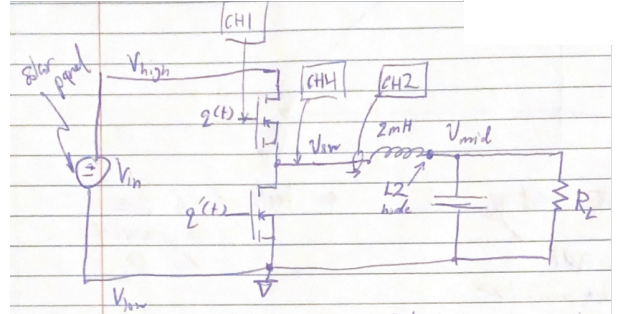


Fig. 13: Circuit schematic for synchronous buck converter.

of $\approx 0.27 \Omega$. The overall setup on the lab bench is shown in Fig. 14

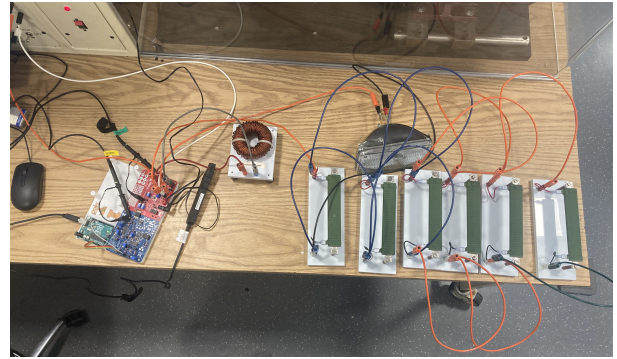


Fig. 14: Setup on lab bench showing power board, Arduino, lamp, and load resistance.

1) Capturing I-V characteristic: The Arduino-based digital controller was set to "mode 4" in which the duty cycle is swept from 0.05 to 0.95. This resulted in the load resistance varying from $400R_L$ to $1.11R_L$.

Since the duty cycle is changed relatively quickly, we can sweep the I-V characteristic while the operating conditions for the PV panel remain essentially constant.

To record data, we used the serial UART on the Arduino to print data to PuTTY with a baud rate of 115200. The following variables were logged:

- PV input voltage V_{in} (V)
 - Output voltage V_{out} (V)
 - Inductor current (A)
 - Duty cycle
 - Output power (W)

2) *MPPT algorithm*: For this part of the experiment, "mode 5" of the Arduino code was turned on, which implements a form of P&O control. The algorithm had two parameters: ΔD and c_{max} . The ΔD controlled how much the duty cycle was stepped each cycle, and the c_{max} value specified the maximum value for a counter which set the period of the perturbation cycles.

The following trials were conducted with varying P&O parameters:

- 1) $\Delta D = 0.01$ and $c_{max} = 1000$
 - 2) $\Delta D = 0.1$ and $c_{max} = 1000$
 - 3) $\Delta D = 0.01$ and $c_{max} = 500$

¹²Answer to study question 3 in lab 11

- 4) $\Delta D = 0.01$ and $c_{max} = 1000$. In this test, a larger dataset was captured, which included instances of manually shading the PV panel.

C. Results

1) *I-V characteristic*: Using the test case with six $2\ \Omega$ resistors in parallel, we captured data over a few minutes and saved it via a PuTTY log.

Since input current I_{in} was not measured directly, we can assume $\eta = 1$ and apply a power balance relationship to get $I_{in} = P_{out}/V_{in}$. We also assume that there are no calibration errors in the Arduino readings.

The results for the I-V characteristic curve and the power vs V_{in} curve are plotted in Fig. 15 and 16.

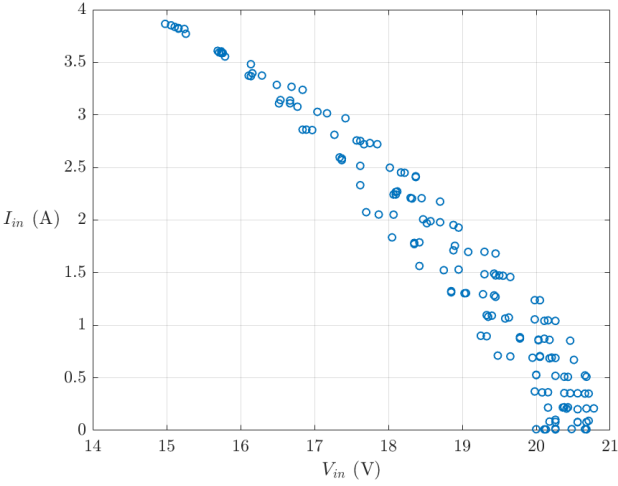


Fig. 15: Measured I-V characteristic for the PV panel. Note that we only get the right-side of the curve, due to the buck topology.

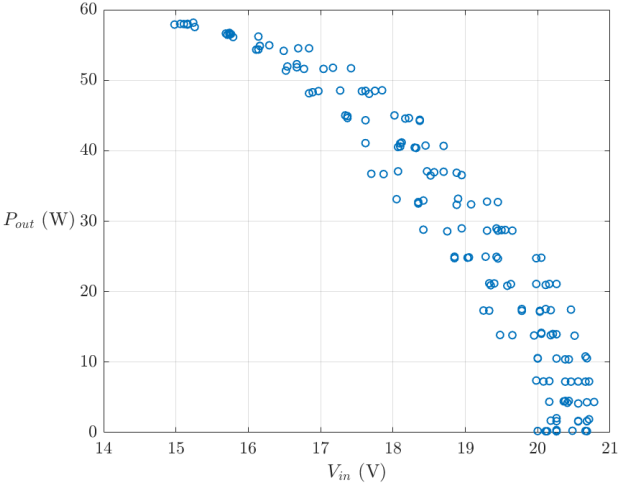


Fig. 16: Measured P vs V curve for the PV panel.

Both of the curves in Fig. 15 and 16 show some spread in the data points, which may be due to slight deviations in solar irradiance during the duration of the data collection.

2) *MPPT results*: On the morning that we conducted experiment 11, there was very little cloud overcast. The sky appeared as shown in Fig. 17

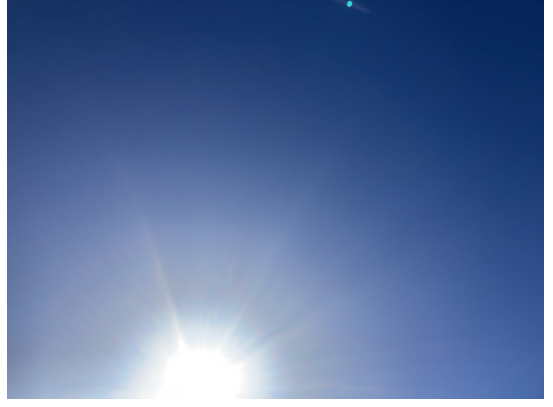


Fig. 17: Photo of sky, taken during experiment 11.

Results for measured P_{out} and D vs log sample are shown in Fig. 18 and 19 for the first three MPPT trials.

Depending on the P&O parameters, the aggressiveness of the MPPT control varied. The first test case (blue line) showed a medium response time, which took around 100 samples to reach the MPP from $D = 0.05$. Increasing the step by a factor x10 improved the response time significantly, as shown in test case 2 (red line). However, oscillations in output power were much more noticeable—we could see flickering in lamp brightness. The last test case (yellow line) had the slowest response time and similar oscillation amplitude.

In the 4th trial, data was logged for an extended period. To emulate cloud cover, we manually shaded the PV panel using a piece of cardboard. Results are shown in Fig. 20 and 21.

Shading resulted in large variations in output power, from 0 to 60 W. Note that, because PuTTY does not timestamp each line of data, we were not able to plot the results versus time. In the future, this issue could be resolved by logging a

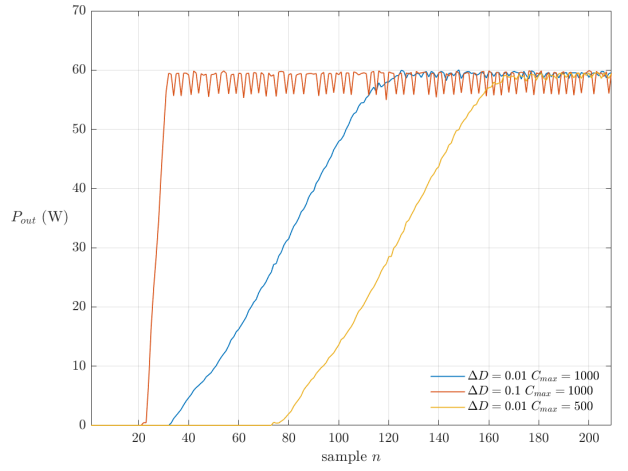


Fig. 18: Output power time-series for first three MPPT test cases.

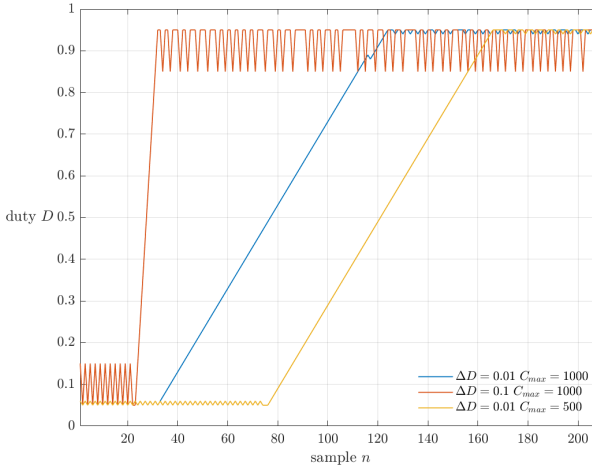


Fig. 19: Duty cycle time-series for first three MPPT test cases.

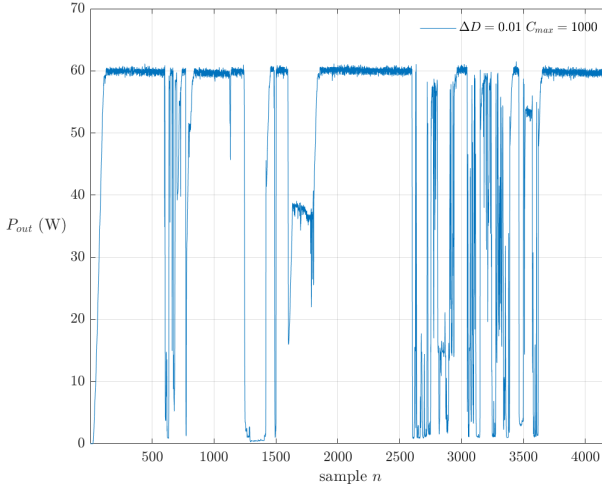


Fig. 20: Output power time-series for 4th test cases.

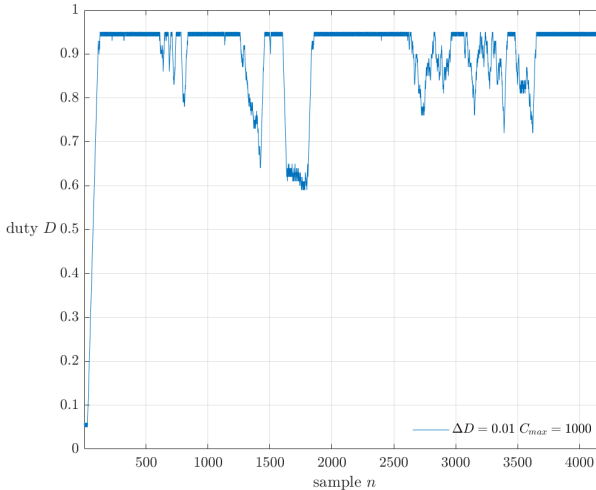


Fig. 21: Duty cycle time-series for 4th test case.



Fig. 22: Scopeshot showing MPPT operation during partial shading of the PV panel. CH1 is $q(t)$, CH2 is the inductor current, and CH4 is $v_{sw}(t)$.

timestamp generated by one of the Arduino's built in timers, e.g., using the MILLIS function.

At around $n = 1750$ samples, the scope-shot shown in Fig. 22 was recorded for partially shaded operation. Here, the MPP exists at $D = 0.62$ and $P_{out} \approx 38$ W.

IV. CONCLUSION

Overall we implemented PWM generation both via analog and digital means and developed digital control to track a reference current and maximum power point for a PV panel. We learned principles of deadtime for operating a synchronous converter and basic feedback control (P, PI, and P&O) as used in DC-DC converters.

REFERENCES

- [1] ECE 469 lab manual
- [2] P. T. Krein and J. A. Galtieri, "Active Management of Photovoltaic System Variability With Power Electronics," *IEEE Journal of Emerging and Selected Topics in Power Electronics*, vol. 9, no. 6, pp. 6507–6523, Dec. 2021, doi: 10.1109/JESTPE.2020.3006448.